10 g body weight) by tail vein injection. The mice were sacrificed 1 day after dye injection. The TA muscles were removed and photographed using a digital camera. The TA muscles were embedded in an OCT compound and immediately frozen at –80°C. Serial sections 10 μm thick were cut by cryostat and observed with a fluorescence microscope (Axiovert 200 M, Carl Zeiss).

Hindlimb Ischemia Model

The ischemic hindlimb model was created in five-week-old male ICR mice as previously reported (26). Briefly, animals were anesthetized, and a skin incision was made in the left hindlimb. After ligation of the proximal end of the femoral artery at the level of the inguinal ligament, the distal portion and all the side branches were dissected free and excised. The right hindlimb was kept intact to control the original blood flow. Immediately after ischemia was induced, a mixture of 40 μl of a pDNA (10 μg of pBLAST-hbFGF or pBLAST as an control vector) and BL (30 μg) suspension was injected into the adductor muscle of the ischemia mice, and US exposure (1 MHz, 2 w/cm^2, 50% duty cycle, 60 s) was immediately applied at the injection site. Measurements of the ischemic (left)/normal (right) limb blood flow ratio were performed for a set time using a laser Doppler blood flow meter (OMEGAFLO, FLO-C1).

bFGF ELISA

bFGF secretion was determined as previously reported (27). Briefly, 5- to 6-week-old male ICR mice were anesthetized by intraperitoneal injection of pentobarbital. The leg was shaved and depilated to expose the tibialis anterior muscle. Ten micrograms of DNA in a 40 μL bubble liposome or PBS solution were injected into the tibialis anterior muscle. After DNA injection, US exposure was applied. The tibialis anterior muscle was collected 2 days after the DNA injection. The muscle was washed three times in 3 mL of PBS to remove debris and blood. The washed muscle was placed in a 24-well plate coating growth factor reduced Matrigel (BD Biosciences) and incubated at 37°C. The muscle was grown in 1.5 mL of M199 medium containing 2% fetal bovine serum, 100 U/mL penicillin, and 100 mg/mL streptomycin. The levels of secreted cytokines in the conditioned media of the explants cultures were measured using human bFGF ELISA (R&D Systems), according to the manufacturer's instructions.

Immunohistochemistry

The ischemic thigh muscles were perfused on day 14 with PBS and 4% paraformaldehyde and embedded in paraffin. Muscle sections (4 μm) were stained with anti-CD31 antibody (BD pharmingen) overnight at 4°C. We then incubated the sections with Alexa Fluor 488 rabbit anti-rat IgG (Molecular Probes).

In Vivo Studies

Animal use and relevant experimental procedures were approved by the Tokyo University of Pharmacy and Life Science Committee and Teikyo University on the Care and Use of Laboratory Animals. All experimental protocols for animal studies were in accordance with the Principle of Laboratory Animal Care in Teikyo University.

Statistical Analyses

All data are shown as the mean±SD (n=4 or 6). Data were considered significant when $P<0.05$. The t-test was used to calculate statistical significance.

RESULTS

In Vivo Gene Delivery into the Skeletal Muscle of Mice with BL and US Exposure

It has been reported that microbubbles improve tissue permeability by cavitation upon US exposure. We first tried to deliver the naked pDNA (pCMV-Luc) into tibialis muscle using BL and US. A solution of pDNA and BL was injected into TA muscle, and US was immediately applied to the injection site, as shown in Fig. 1. As a result, the relative luciferase activity was high in the group treated using the pDNA plasmid with BL and US exposure. In contrast, there was low activity in the groups treated with pDNA alone, pDNA+BL, or pDNA+US. The luciferase activity in the group receiving a combination of BL with US exposure was 200- or 20-fold higher than that of the group treated with pDNA alone or pDNA + US, respectively (Fig. 1a). We next investigated whether their gene expression was derived from muscle cells. In a similar fashion, the EGFP expression plasmid (pEGFP-N3) was delivered into TA muscle, and 5 days after the gene delivery, the EGFP expression was sectioned and examined by fluorescent microscopy. As shown in Fig. 1b, the intramuscular gene delivery of the EGFP expression plasmid by BL and US exposure was present in a wide area of the positive muscle fibers of EGFP. In contrast, in the muscle specimens of the other treated groups (pDNA alone, pDNA+BL, or pDNA+US), very little expression was shown (Fig. 1b). We also observed the luciferase gene expression area in the whole body using an *in vivo* luciferase imaging system at 5 days after the transfection into the muscle treated with pDNA, BL, and US exposure.

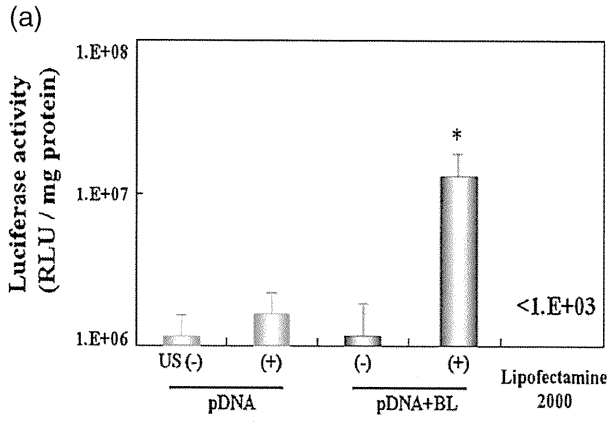

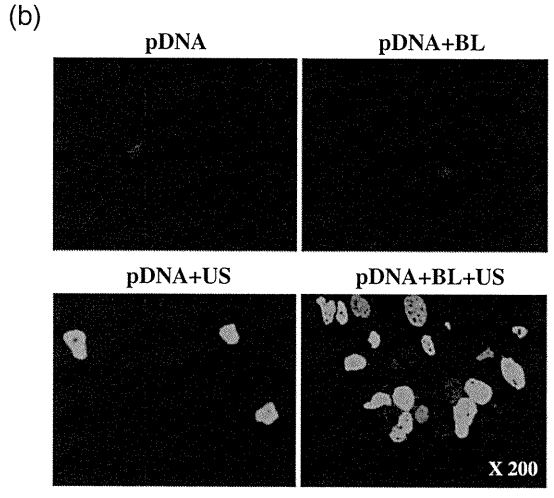

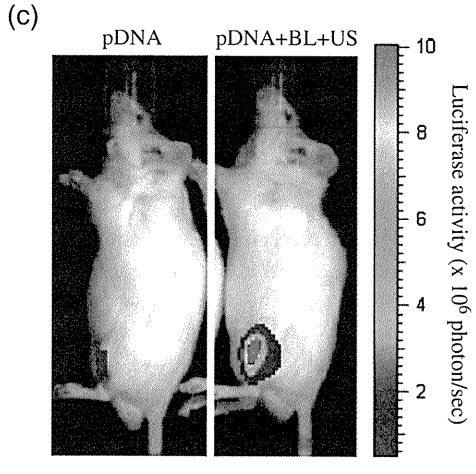

◀ **Fig. 1** Reporter gene expression after BL and US-mediated gene transfer compared with Lipofectamine 2000. (a) Luciferase expression after BL and US-mediated gene transfer compared with Lipofectamine 2000. Mice were treated with BL and US-mediated intramuscular luciferase gene transfer or Lipofectamine 2000. Five days after transfection, luciferase expression was determined. In another experiment, a pDNA (pCMV-Luc (10 μg))-Lipofectamine 2000 (25 μg) complex was suspended in PBS and injected into the left femoral artery. *$P < 0.01$ compared to the group of pDNA alone, pDNA + US, pDNA + BL, or Lipofectamine 2000 with BL. pDNA (pCMV-Luciferase): 10 μg, BL: 30 μg. US exposure (Frequency: 1 MHz, Duty: 50%, Intensity: 2 W/cm^2, Time: 60 s). (b) EGFP expression after BL and US-mediated gene transfer. Mice were treated with BL and US-mediated intramuscular EGFP gene transfer. Five days after transfection, EGFP expression was analyzed by fluorescent microscopy. Each of the gene transfer conditions are indicated above the pictures. Magnification: x 200. (c) photon counts are indicated by the pseudo-color scales.

Although the level of gene expression gradually decreased 2 weeks after the transfection using BL and US exposure, the moderate gene expression persisted for 4 weeks after the transfection (data not shown). The gene expression was restricted to the area of US exposure (Fig. 1c). This suggested that the combination of BL and US exposure facilitated the efficient transfection of pDNA into the muscle due to the induction of cavitation. We also assessed the tissue damage by testing EBD uptake in the muscle transfected with the BL and US exposure; however, significant tissue damage was not observed at the US condition (frequency: 1 MHz; duty: 50%; intensity: 2 W/cm^2; time: 60 s), even in the presence of the cavitation by BL and US exposure (Fig. 2b, e). When a higher US intensisty (4 W/cm^2) was applied, significant tissue damage was detected (Fig. 2c, f).

In Vivo Effects of the bFGF Expression System

We next attempted to deliver bFGF plasmid into tibialis muscle using BL and US and determine the bFGF protein expression in explant culture medium. The amount of bFGF protein was high in the group treated with bFGF plasmid with BL and US exposure. In contrast, there was low expression in the group treated with bFGF plasmid alone, or bFGF plasmid+US (Fig. 3). We further investigated the capillary density in order to know the effects of BL and US-mediated gene delivery with bFGF plasmid injected intramuscularly into hindlimb ischemia model mice. In the treatment group with BL and US-mediated gene transfer, their capillary vessels with CD31 positive cells were significantly increased compared to the treatment group of the control plasmid (empty vector), the bFGF plasmid alone, or bFGF plasmid + US (Fig. 4a, b). Measurements of the ischemic (left)/non-ischemic (right) hindlimb blood flow ratio were further performed for a period of time using a laser Doppler blood flow meter. Consistent with this induction of angiogenesis, the blood flow in the group treated with the bFGF plasmid with BL and US exposure was significantly increased compared with the group treated with the control plasmid (empty vector), the bFGF plasmid alone, bFGF plasmid + US (Fig. 5). Although we also examined the blood flow ratio after treatment with US exposure alone or BL with US exposure

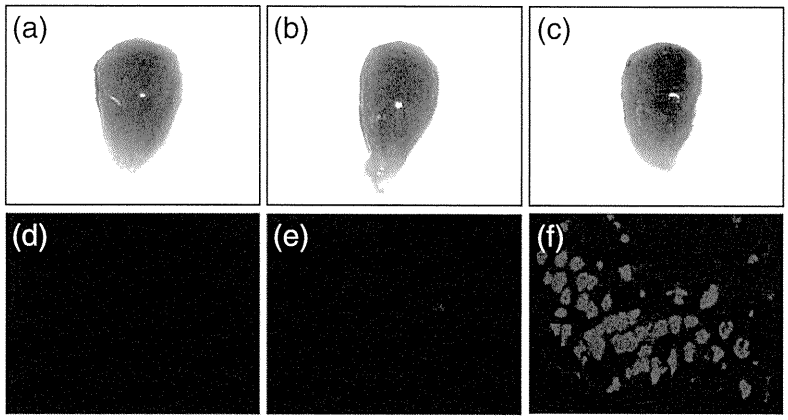

Fig. 2 Tissue-damage testing using EBD. pDNA alone without BL and US exposure (a, d). pDNA with BL and US exposure condition at a frequency of 1 MHz with an intensity of 2 W/cm^2 (b, e), or 4 W/cm^2 (c, f) for 60 s. The TA muscles were photographed using a digital camera (a, b, and c). Evans-blue fluorescence of 10 μm cryosections from the TA muscles was examined with fluorescence microscopy (d, e, and f). Magnification: ×100.

to the ischemic limb muscle, their blood flow ratio still remained in the 20 to 40% range. These results suggest that intramuscular injection of bFGF as an angiogenic gene with bubble liposomes followed by US exposure enabled us to improve an angiogenesis in the ischemic muscle.

DISCUSSION

The gene delivery of naked plasmid DNA is a feasible technique for non-viral gene therapy in a safe clinical use; however, a higher efficiency of site-specific delivery is required to achieve therapeutic effects in patients. In this view, we previously reported that BL is an efficient gene delivery tool (24,28,29). However, it is not enough to say that BL is a feasible and effective tool to carry out gene therapy to treat diseases. Here we demonstrate the development of a safe and efficient gene delivery system into skeletal muscle using the combination of BL and US exposure, and we assess the feasibility and the effectiveness of BL for angiogenic gene delivery. We therefore examined the potential ability of BL with US exposure to deliver a gene into skeletal muscle and its applicability for therapeutic angiogenesis in ischemic model. By using BL with US exposure, we first performed a transfer of luciferase-expressing plasmid DNA as a reporter plasmid into the TA muscle of mice. The remarkable gene expression could be enhanced efficiently only with the combination of both BL and US exposure when compared with other treatments (Fig. 1a). Exceeding our expectations, their gene expression was 200-fold higher than that of the plasmid DNA injection alone. When compared to Optison, one of the currently existing microbubbles (9–11), with US exposure, however, the gene transfer efficacy of BL was almost same as when using Optison (data not shown). Previously, our reports have demonstrated that the gene transfection efficiency *in vitro* could be affected with increasing the US intensity and the exposure time (20). The transfection efficiency increased with an increasing intensity of ultrasound and reached a plateau at 2 W/cm^2. No significant damage was observed under these conditions (Fig. 2b, e). When a higher intensity of US (4 W/cm^2) during the gene transfer with BL was applied to improve the transfection efficiency, the gene expression was conversely diminished (data not shown), and significant damage was also observed (Fig. 2c, f). This treatment caused significant tissue damage, probably due to the temperature elevation in the US exposure site. In this experiment, we therefore employed an US condition (frequency: 1 MHz; intensity: 2 W/cm^2; duty cycle: 50%; US exposure time: 1 min) that was in terms with a safety profile. As shown in Fig. 1b, the number of EGFP-positive muscle fibers could be apparently enhanced by the combination of BL and US

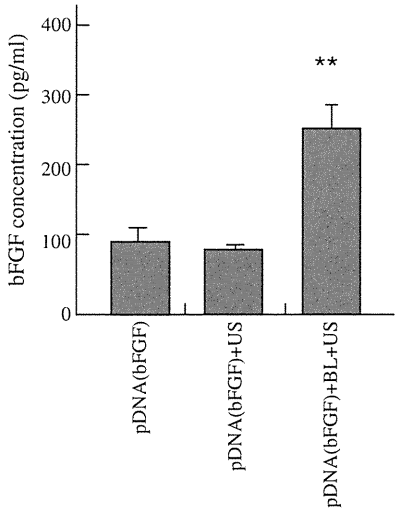

Fig. 3 bFGF protein expression after BL and US-mediated bFGF gene transfer. Mice were treated with BL and US-mediated intramuscular bFGF gene transfer. Two days after transfection, the muscle was collected and placed into Matrigel coating plates. After 3 days, the secreted bFGF protein expression was determined by ELISA. $^{**}P<0.05$ *vs.* other treatment groups. pDNA (pBLAST-bFGF): 10 μg, BL: 30 μg, US exposure (Frequency: 1 MHz, Duty: 50%, Intensity: 2 W/cm^2, Time: 60 s).

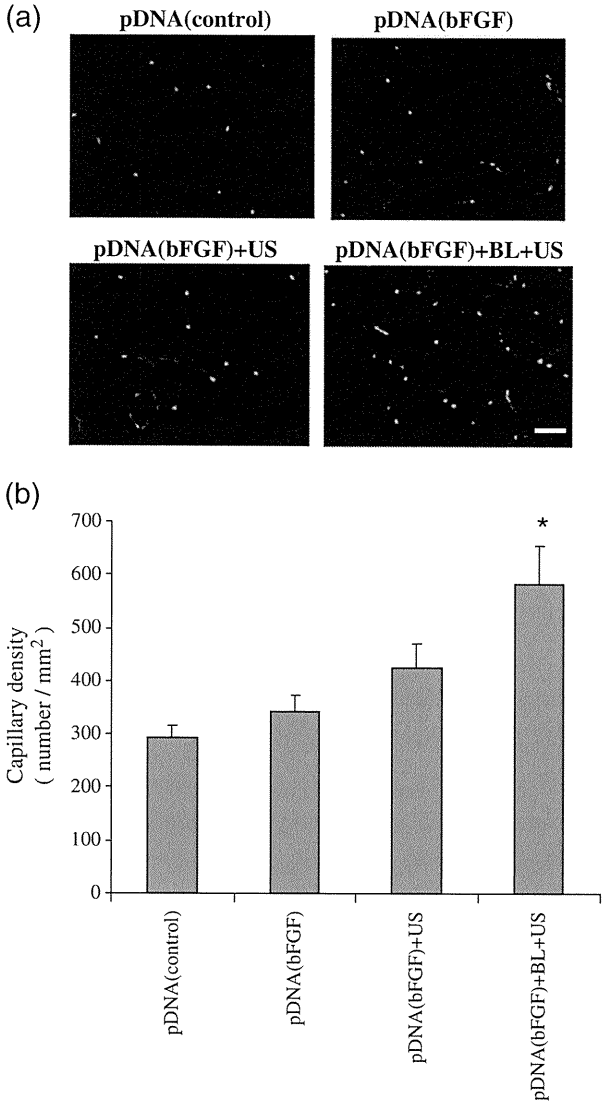

Fig. 4 Effect of BL and US-mediated bFGF gene transfer into hindlimb ischemia on capillary density. (a) CD31 staining of hindlimb muscle sections 14 days after BL and US-mediated bFGF gene transfer. The stained sections were analyzed by fluorescent microscopy. (b) CD31 positive vessels were measured. Green dots indicate CD31 positive vessels stained with an FITC-labeled anti-CD31 antibody. Scale bar represented 50 μm. *$P < 0.05$ *vs.* other treatment groups.

exposure; in contrast, without BL, only a few fibers could be observed in a treatment of US exposure without BL. Consequently, we found that a gene delivery method using BL and US exposure helped to both improve the transfection efficiency in the US focused site with a minimally invasive transfection procedure.

It is unclear whether BL with US exposure could improve transgene expression. Previously, we reported that BL could induce cavitation by a short duration (1–10 s) of US exposure and lead to efficient gene transfer into various types of cells (19,20). Therefore, the major biological effect of BL for gene delivery into the muscle may be through a cavitation induction, as was shown in previous reports (19). In contrast, in the case of Lipofectamine 2000, a commercial cationic lipid that is widely used in gene delivery, the transfection efficiency in the muscle was markedly lowered (Fig. 1a). This result is consistent with reports that serum proteins interact with and disturb cationic liposomes (29). It is expected that more time is required for this transfection, because cationic lipid/pDNA complexes (lipoplex) are entered into the cytoplasm by an endosomal pathway. Therefore, when the lipoplex with Lipofectamine 2000 was directly injected into the muscle, before it could enter into the cytoplasm by an endosomal pathway, it is possible that the degradation of pDNA or the aggregation of lipoplexes easily occurred. In contrast, once a solution of both BL and pDNA is administered into the muscle, US exposure is immediately applied at the injection site, leading to efficient gene expression, as shown in Fig. 1. In this way, unlike with lipoplexes, this simple method with BL and US exposure does not require a long time to achieve an efficient gene transfection. Our previous report has demonstrated that, by BL and US exposure, siRNA could directly enter into the cytoplasm without an endosomal pathway (22). In this report, because the level of gene expression corresponding

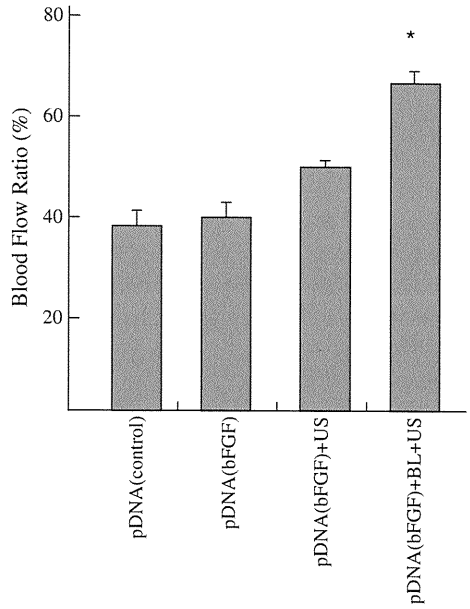

Fig. 5 Effect of BL and US-mediated bFGF gene transfer on the recovery of blood flow in ischemic limbs. After femoral artery ligation, mice were treated with BL and US-mediated intramuscular bFGF gene transfer. After the transfection, blood flow was measured at 14 days using a laser Doppler blood flow meter. *$P < 0.05$ *vs.* other treatment groups. Blood Flow Ratio (%): ischemic / normal blood flow ratio. pDNA (pBLAST-bFGF): 10 μg, BL: 30 μg, US exposure (Frequency: 1 MHz, Duty: 50%, Intensity: 2 W/cm^2, Time: 60 s).

to half of the expression in BL with a 1-minute US exposure could also be observed by BL with an only 10-second US exposure (data not shown), it may be thought that this transfection method by BL with US exposure enables immediate and direct pDNA delivery into the cytoplasm of muscle cells. The transfection efficiency might increase due to the appearance of transient holes in the cell membrane caused by the spreading of the BL, followed by their eruption with US exposure, which is consistent with previous reports using Optison (9).

Recently, a therapeutic strategy delivering angiogenic gene factors has been widely studied for clinical use in ischemic diseases (30). The delivery of naked plasmid DNA encoding an angiogenic gene into the ischemia has also been reported in clinical trials. However, the transfection efficiency is still insufficient for effective angiogenesis without side effects (30). Therefore, we assessed the feasibility and the effectiveness of BL for a gene therapy by trying to deliver a plasmid expressing bFGF, a key angiogenic factor, into the skeletal muscle of hindlimb ischemia model mice by the combination of BL and US exposure. As expected, with the gene delivery of the bFGF plasmid into an intramuscular injection with the combination of BL and US exposure, the capillary density and the blood flow ratio of the ischemic to non-ischemic hindlimb were markedly increased in the hindlimb transfected with the bFGF plasmid DNA through the combination of BL and a low intensity of US exposure compared to the plasmid DNA injection alone (Figs. 4 and 5). In addition, it has been reported that low-intensity US exposure can induce angiogenesis (31,32). However, no significant recovery in ischemic hindlimbs was observed with the combination of BL and US exposure without bFGF plasmid or with US exposure alone without the bFGF plasmid (data not shown). These results apparently indicate that therapeutic angiogenesis using naked plasmid DNA transfer that is enhanced by BL and US exposure could be a potential method in a clinical setting. We believe that there are several possibilities for BL usage in therapeutic angiogenesis with naked plasmid DNA in clinical use. The novel method using the combination of BL and US exposure may possibly reduce the amount of naked plasmid DNA, administration times, and the achievement of efficient gene transfer non-invasively without a viral vector, thereby enabling the decrease of the potential cost in clinical settings.

CONCLUSION

The present studies demonstrated a novel gene delivery method into skeletal muscle by the combination of BL and US exposure. Applied as gene therapy in a mouse model of ischemic limb muscle, intramuscular injection of bFGF as an angiogenic gene with BL followed by US exposure enabled improvement of an angiogenesis followed by apparent increased blood flow in the ischemic muscle. Because intramuscular injection of naked plasmid DNA alone may be inefficient and restrict its clinical use, this US-mediated BL technique may provide an effective non-invasive and non-viral method for angiogenic gene therapy for limb ischemia as well as for wound healing, ischemic heart disease, myocardial infarction, peripheral arterial diseases, and other various diseases.

ACKNOWLEDGEMENTS

We are grateful to Dr. Katsuro Tachibana (Department of Anatomy, School of Medicine, Fukuoka University) for technical advice regarding the induction of cavitation with US and to Mr. Yasuhiko Hayakawa, Mr. Takahiro Yamauchi, and Mr. Kosho Suzuki (NEPA GENE CO., LTD.) for technical advice regarding US exposure. This study was supported in part by the Industrial Technology Research Grant Program (04A05010) from New Energy, the Industrial Technology Development Organization (NEDO) of Japan, Grant-in-Aid for Scientific Research (B) (20300179) from the Japan Society of the Promotion of Science, and by a grant for private universities provided by the Promotion and Mutual Aid Corporation for Private Schools of Japan.

REFERENCES

1. Miller DG, Rutledge EA, Russell DW. Chromosomal effects of adeno-associated virus vector integration. Nat Genet. 2002;30:147–8.
2. Fechheimer M, Boylan JF, Parker S, Sisken JE, Patel GL, Zimmer SG. Transfection of mammalian cells with plasmid DNA by scrape loading and sonication loading. Proc Natl Acad Sci U S A. 1987;84:8463–7.
3. Miller MW, Miller DL, Brayman AA. A review of in vitro bioeffects of inertial ultrasonic cavitation from a mechanistic perspective. Ultrasound Med Biol. 1996;22:1131–54.
4. Joersbo M, Brunstedt J. Protein synthesis stimulated in sonicated sugar beet cells and protoplasts. Ultrasound Med Biol. 1990;16:719–24.
5. Greenleaf WG, Bolander ME, Sarkar G, Goldring MB, Greenleaf JF. Artificial cavitation nuclei significantly enhance acoustically induced cell transfection. Ultrasound Med Biol. 1998;24:587–95.
6. Schratzberger P, Krainin JG, Schratzberger G, Silver M, Ma H, Kearney M, *et al.* Transcutaneous ultrasound augments naked DNA transfection of skeletal muscle. Mol Ther. 2002;6:576–83.
7. Duvshani-Eshet M, Machluf M. Therapeutic ultrasound optimization for gene delivery: a key factor achieving nuclear DNA localization. J Control Release. 2005;108:513–28.
8. Kim HJ, Greenleaf JF, Kinnick RR, Bronk JT, Bolander ME. Ultrasound-mediated transfection of mammalian cells. Hum Gene Ther. 1996;7:1339–46.

9. Taniyama Y, Tachibana K, Hiraoka K, Aoki M, Yamamoto S, Matsumoto K, *et al.* Development of safe and efficient novel nonviral gene transfer using ultrasound: enhancement of transfection efficiency of naked plasmid DNA in skeletal muscle. Gene Ther. 2002;9:372–80.
10. Taniyama Y, Tachibana K, Hiraoka K, Namba T, Yamasaki K, Hashiya N, *et al.* Local delivery of plasmid DNA into rat carotid artery using ultrasound. Circulation. 2002;105:1233–9.
11. Li T, Tachibana K, Kuroki M, Kuroki M. Gene transfer with echo-enhanced contrast agents:comparison between Albunex, Optison, and Levovist in mice–initial results. Radiology. 2003;229:423–8.
12. Unger EC, Porter T, Culp W, Labell R, Matsunaga T, Zutshi R. Therapeutic applications of lipid-coated microbubbles. Adv Drug Deliv Rev. 2004;56:1291–314.
13. Sonoda S, Tachibana K, Uchino E, Okubo A, Yamamoto M, Sakoda K, *et al.* Gene transfer to corneal epithelium and keratocytes mediated by ultrasound with microbubbles. Invest Ophthalmol Vis Sci. 2006;47:558–64.
14. Blume G, Cevc G. Liposomes for the sustained drug release in vivo. Biochim Biophys Acta. 1990;1029:91–7.
15. Allen TM, Hansen C, Martin F, Redemann C, Yau-Young A. Liposomes containing synthetic lipid derivatives of poly(ethylene glycol) show prolonged circulation half-lives in vivo. Biochim Biophys Acta. 1991;1066:29–36.
16. Maruyama K, Yuda T, Okamoto A, Kojima S, Suginaka A, Iwatsuru M. Prolonged circulation time in vivo of large unilamellar liposomes composed of distearoyl phosphatidylcholine and cholesterol containing amphipathic poly(ethylene glycol). Biochim Biophys Acta. 1992;1128:44–9.
17. Maruyama K, Ishida O, Kasaoka S, Takizawa T, Utoguchi N, Shinohara A, *et al.* Intracellular targeting of sodium mercaptoundecahydrododecaborate (BSH) to solid tumors by transferrin-PEG liposomes, for boron neutron-capture therapy (BNCT). J Control Release. 2004;98:195–207.
18. Negishi Y, Omata D, Iijima H, Hamano N, Endo Y, Suzuki R, Maruyama K, Nomizu M, and Aramaki Y, Preparation and Characterization of Laminin-derived Peptide AG73-coated Liposomes as a Selective Gene Delivery Tool. *Biol Pharm. Bull. in press*
19. Suzuki R, Takizawa T, Negishi Y, Hagisawa K, Tanaka K, Sawamura K, *et al.* Gene delivery by combination of novel liposomal bubbles with perfluoropropane and ultrasound. J Control Release. 2007;117:130–6.
20. Suzuki R, Takizawa T, Negishi Y, Utoguchi N, Sawamura K, Tanaka K, *et al.* Tumor specific ultrasound enhanced gene transfer in vivo with novel liposomal bubbles. J Control Release. 2008;125:137–44.
21. Suzuki R, Takizawa T, Negishi Y, Utoguchi N, Maruyama K. Effective gene delivery with novel liposomal bubbles and ultrasonic destruction technology. Int J Pharm. 2008;354:49–55.
22. Negishi Y, Endo Y, Fukuyama T, Suzuki R, Takizawa T, Omata D, *et al.* Delivery of siRNA into the cytoplasm by liposomal bubbles and ultrasound. J Control Release. 2008;132:124–30.
23. Negishi Y, Omata D, Iijima H, Takabayashi Y, Suzuki K, Endo Y, *et al.* Enhanced laminin-derived peptide AG73-mediated liposomal gene transfer by bubble liposomes and ultrasound. Mol Pharm. 2010;7:217–26.
24. Suzuki R, Namai E, Oda Y, Nishiie N, Otake S, Koshima R, *et al.* Cancer gene therapy by IL-12 gene delivery using liposomal bubbles and tumoral ultrasound exposure. J Control Release. 2010;142:245–50.
25. Liu F, Huang L. A syringe electrode device for simultaneous injection of DNA and electrotransfer. Mol Ther. 2002;5:323–8.
26. Couffinhal T, Silver M, Zheng LP, Kearney M, Witzenbichler B, Isner JM. Mouse model of angiogenesis. Am J Pathol. 1998;152:1667–79.
27. Jang HS, Kim HJ, Kim JM, Lee YS, Kim KL, Kim JA, *et al.* A novel *ex Vivo* angiogenesis assay based on electroporation-mediated delivery of naked plasmid DNA to skeletal muscle. Mol Ther. 2004;9:464–74.
28. Koch S, Pohl P, Cobet U, Rainov NG. Ultrasound enhancement of liposome-mediated cell transfection is caused by cavitation effects. Ultrasound Med Biol. 2000;26:897–903.
29. Yang JP, Huang L. Overcoming the inhibitory effect of serum on lipofection by increasing the charge ratio of cationic liposome to DNA. Gene Ther. 1997;4:950–60.
30. Shah PB, Losordo DW. Non-viral vectors for gene therapy: clinical trials in cardiovascular disease. Adv Genet. 2005;54:339–61.
31. Emoto M, Tachibana K, Iwasaki H, Kawarabayashi T. Antitumor effect of TNP-470, an angiogenesis inhibitor, combined with ultrasound irradiation for human uterine sarcoma xenografts evaluated using contrast color Doppler ultrasound. Cancer Sci. 2007;98:929–35.
32. Barzelai S, Sharabani-Yosef O, Holbova R, Castel D, Walden R, Engelberg S, *et al.* Low-intensity ultrasound induces angiogenesis in rat hind-limb ischemia. Ultrasound Med Biol. 2006;32:139–45.

International Journal of Cardiology 152 (2011) 202–206

Contents lists available at ScienceDirect

International Journal of Cardiology

journal homepage: www.elsevier.com/locate/ijcard

Enhancement of ultrasonic thrombus imaging using novel liposomal bubbles targeting activated platelet glycoprotein IIb/IIIa complex—*in vitro* and *in vivo* study

Kohsuke Hagisawa [a], Toshihiko Nishioka [b,*], Ryo Suzuki [c], Tomoko Takizawa [c], Kazuo Maruyama [c], Bonpei Takase [d], Masayuki Ishihara [d], Akira Kurita [d], Nobuo Yoshimoto [b], Fumitaka Ohsuzu [e], Makoto Kikuchi [a]

[a] *Department of Medical Engineering, National Defense Medical College, 3-2 Namiki, Tokorozawa, Saitama 359-8513, Japan*
[b] *Division of Cardiology, Saitama Medical Center, Saitama Medical University, 1981 Kamoda, Kawagoe, Saitama 350-8550, Japan*
[c] *Department of Biopharmaceutics, School of Pharmaceutical Science, Teikyo University, 1091-1 Suwarashi, Sagamiko, Sagamihara, Kanagawa 229-0195, Japan*
[d] *Division of Biomedical Engineering, National Defense Medical College, 3-2 Namiki, Tokorozawa, Saitama 359-8513, Japan*
[e] *First Department of Internal Medicine, National Defense Medical College, 3-2 Namiki, Tokorozawa, Saitama 359-8513, Japan*

ARTICLE INFO

Article history:
Received 12 February 2010
Received in revised form 19 June 2010
Accepted 4 July 2010
Available online 1 August 2010

Keywords:
Echocardiography
Thrombus
Imaging
Ultrasound
Liposome

ABSTRACT

Background: We developed perfluorocarbon gas-containing bubble liposomes (BL) with Arg-Gly-Asp (RGD) sequence-containing peptides, which bind to activated platelet glycoprotein IIb/IIIa complexes. The aim of this study was to examine the enhancing effects in ultrasonic thrombus imaging using these targeted BL *in vitro* and *in vivo*.

Methods: Liposomes composed of phosphatidylcholine and cholesterol were manufactured, and RGD peptide was attached by a covalent coupling reaction. Sonication was used to conjugate liposomes and perfluorocarbon gas, which formed targeted BL. *In vitro*, targeted BL were mixed with whole blood, which was allowed to coagulate while being shaken and rotated. *In vivo*, we administered targeted BL to 10 rabbits with acute thrombotic occlusions in the ilio-femoral artery. Thrombi were imaged using a 7.5–9 MHz linear transducer and a conventional ultrasound machine, and by scanning electron microscopy. Ultrasound images were digitized, and mean pixel gray-scale level (black = 0, white = 255) was measured.

Results: In vitro, mean pixel gray-scale level of the thrombi in targeted BL group was significantly higher than in control and non-targeted BL groups (93 ± 26 vs. 58 ± 16, 48 ± 9, $p = 0.002$, $n = 10$). Scanning electron microscopy revealed large amounts of targeted BL attached to the thrombi. *In vivo*, mean pixel gray-scale level of the thrombi with targeted BL was significantly higher (33.2 ± 6.4 vs. 24.8 ± 8.5, $p = 0.0051$, $n = 10$) than that before targeted BL administration.

Conclusions: Perfluorocarbon gas-containing BL with RGD peptide represent a novel echo contrast agent, which can markedly enhance ultrasonic thrombus imaging *in vitro* and *in vivo*, and may be useful for noninvasively diagnosing acute thrombotic vessel occlusion.

1. Introduction

Echocardiographic diagnosis of vascular or intracardiac thrombi is sometimes challenging, even using state-of-the-art ultrasound systems and comercially available ultrasound contrast agents [1,2]. Intravascular ultrasound imaging provides more detailed pictures of thrombi due to its higher frequency; however, thrombi within the vessel lumen can often be mistaken for soft plaques, unless they are distinguished from soft plaques by mobility, lobular edges and movement away from the vessel wall during the cardiac cycle [3]. Therefore, it is essential to improve the diagnostic accuracy of echocardiography for detecting thrombi *in vivo*.

Recently, using emerging molecular imaging techniques, several types of novel thrombus-targeting ultrasound contrast agents have been developed and examined for use in the diagnosis of thrombi *in vitro* and in animal models [4–10]. These ultrasound contrast agents are lipid-encapsulated perfluorocarbon gas or nongaseous liposomes, and antibodies or peptides are used as specific ligands to fibrin or platelets. However, these agents are not commercially available.

We have developed novel polyethylene glycol-modified liposomal bubbles (bubble liposomes, BL) containing perfluoropropane gas, which can be used as an ultrasound contrast agent [11–13]. We attached targeted ligands for activated platelets to these BL. We used Arg-Gly-Asp (RGD) sequence-containing peptides, which bind to the

* Corresponding author. Tel.: +81 49 228 3587; fax: +81 49 226 5274.
E-mail address: nishioka@saitama-med.ac.jp (T. Nishioka).

0167-5273/$ – see front matter © 2010 Elsevier Ireland Ltd. All rights reserved.
doi:10.1016/j.ijcard.2010.07.016

fibrinogen receptor on the activated platelet membrane glycoprotein IIb/IIIa complex [14–17]. We hypothesized that the activated thrombus-targeting BL would enhance fresh thrombus visualization by conventional transcutaneous ultrasound and may enable diagnosis of acute thrombotic vessel occlusion. The aim of this study was to examine the enhancing effects on ultrasonic imaging of fresh thrombi using these BL *in vitro* and *in vivo*.

2. Materials and methods

2.1. Preparation of thrombus-targeting BL

The lipid-based shell of the perfluorocarbon gas-containing BL was composed of 12.6 mg of 1,2-distearoyl-sn-glycero-phosphatidylcholine (DSPC) (NOF Corp., Tokyo, Japan), 5.1 mg of 1,2-distearoyl-sn-glycero-3-phosphatidyl-ethanolamine-m-poly-ethyleneglycol 2000 maleimide (DSPE-PEG-Mal-2000; Avanti, Alabaster, AL) and 3.0 mg of cholesterol (Sigma-Aldrich Japan, Tokyo, Japan). Liposomes were prepared by reverse phase evaporation [16]. Briefly, a mixture of all reagents was dissolved in 2.0 ml of chloroform and mixed with the same amount of di-isopropyl ether and normal saline. The mixture was sonicated using a probe-type 19.5-kHz ultrasound at 550 W (XL-2020 Sonicator, Misonix, Inc., Farmingdale, NY) and then evaporated at 65 °C using a rotary evaporating system (Tokyo Rika, Tokyo, Japan). After the chemical solvent was completely removed, the size of liposomes was adjusted to be less than 0.2 μm using extruding equipment and a membrane filter (Northern Lipids, Inc., Vancouver, Canada) with sizing filters. To the liposome liquid, 1 mg of linear octapeptide with an amino acid sequence of cysteine–glycine–glycine–glycine–arginine–glycine–aspartic acid–phenyl-alanine (CGGGRGDF) (Operon Biotechnologies, Tokyo, Japan) was added [14,17] and allowed to conjugate to the maleimide on the liposomal surface via thio-ether covalent coupling at room temperature for 2 h. Gel filtration was then used to remove unreacted peptide fragments. Lipid concentration was measured with the Wako Phospholipid C test (Wako Pure Chemical Industries, Osaka, Japan) and the RGD-liposomes were diluted to a final concentration of 20 mg/ml. The RGD-liposomes were sealed in a 5-ml vial and air was exchanged with perfluoropropane gas (Takachiho Chemical Ind. Co., Ltd., Tokyo, Japan), followed by 20-kHz ultrasound treatment using a bath-type sonicating system (Branson model 3510, Emerson, CT) for 5 min to generate RGD-BL [11,12]. Sterilized filtration (0.45 μm) was then performed to remove expanded and oversized BL. Non-targeted BL were also prepared in the same manner, except without the addition of RGD peptides. The diameter of each BL was determined by dynamic laser light-scattering measurements using the ELS-800 particle analyzer (Otsuka Electronics, Osaka, Japan).

2.2. In vitro thrombus imaging

In total, 30 thrombi were used in this *in vitro* study. For preparation of each thrombus, 9 ml of whole blood was collected in a test tube from a healthy volunteer, placed on a seesaw-type shaker and allowed to coagulate at room temperature while being shaken and rotated at a speed of 60 rpm for 1 h. Ten thrombi served as controls, non-targeted BL were added to 10 thrombi and targeted BL were added to the remaining 10 thrombi. Targeted BL or non-targeted BL (100 μl, 20 mg/ml lipid concentration) were added to the test tube after 10 min. The formed thrombi were washed with normal saline, cut into small pieces and placed in a latex tube filled with degassed water. Thrombi were imaged using a 7.5-MHz linear transducer with a conventional ultrasound machine (SONOS2000, Philips Medical Systems, Potomac, MD) (frame rate, 40–50/s; mechanical index, 0.4) in a bath filled with degassed water. As a control, 10 thrombi prepared without BL were also imaged at the same gain setting and ultrasound intensity. For quantitative analysis, the mean video intensity level of whole thrombi was measured on a 256 gray-scale level (black = 0, white = 255) using NIH image software [18].

2.3. Scanning electron microscopic observation of thrombi

Thrombi were prepared as described for the *in vitro* thrombus imaging study. Thrombi with targeted BL, non-targeted BL or saline were fixed in 2% glutaraldehyde in normal saline and dehydrated in a graded ethanol series. Thrombi were further cut and divided into smaller pieces in order to observe the inside as well as the surface. This was followed by critical-point drying and gold sputtering (JEOL JFC-1100, Nippon Denshi, Tokyo, Japan). Specimens were then examined with a conventional scanning electron microscope (JOEL Carry Scope, Nippon Denshi, Tokyo, Japan) at an acceleration voltage of 5 to 15 kV [19].

2.4. Acute thrombotic occlusion model of rabbit ilio-femoral artery

This study followed the American Physiological Society Guidelines for Animal Research, which conform to the "Position of the American Heart Association on Research Animal Use" adopted by the AHA in November 1984. A total of 20 New Zealand white rabbits were used; 10 each for the targeted BL study and the non-targeted BL study. Each rabbit was anesthetized using 50 mg of ketamine and 20 mg of xylazine. Anesthesia was maintained with pentbarbitrate (15 mg/kg). A 5-Fr sheath was inserted into the right carotid artery, a balloon catheter was advanced to the ilio-femoral artery, and the intima was injured by balloon inflation. Afterwards, the balloon catheter was pulled back, a 0.014-inch guide wire was positioned at the injury site, and electrical stimulation (from a 3-V battery) was applied between the guide wire and skin electrode [20,21]. After 30 min, the artery was thrombotically occluded and arterial occlusion was confirmed by angiography.

2.5. In vivo thrombus imaging

The thrombus was imaged in a longitudinal axis view using a 9-MHz linear transducer and a conventional ultrasound machine (UF-750XT, Fukuda Denshi, Ltd., Tokyo, Japan) (frame rate, 24–30/s; mechanical index, 0.3). Manipulating the transducer just above the angiographic vessel occlusion site, the ultrasonic occlusion site was identified as an abrupt interruption of echo-Doppler signal within the vessel. The region of interest was then defined as the area between the near and far vessel walls without a Doppler signal, according to the consensus of two cardiologists (K.H. and T.N.). To maintain the same view, the ultrasound transducer was fixed with a hand-free stabilizer. The ultrasound thrombus images were continuously recorded from just before to 10 min after the bolus injection of targeted BL (1 ml, 20 mg/ml lipid concentration) through the ear vein in 10 rabbits. After the experiment, the video intensity of the thrombus was measured using NIH image, as described for the *in vitro* study. As controls, the video intensity of the thrombi was measured before and after injection of 1 ml (20 mg/ml lipid concentration) of non-targeted (without RGD peptide) BL in another 10 rabbits.

2.6. Statistical analyses

Results are given as means ± 1 standard deviation. As video intensity levels of the thrombi were not considered to be normally distributed, non-parametric tests were used to compare data. For the *in vitro* study, thrombus echo intensity was compared and analyzed using the Kruskal–Wallis test followed by a post-hoc Bonferroni test. For the *in vivo* study, thrombus echo intensity before and after BL administration was compared by the Wilcoxon-signed rank sum test. A p value <0.05 was considered statistically significant.

3. Results

3.1. In vitro thrombus imaging

Ultrasonic images of thrombi were apparently enhanced when compared to the control and non-targeted BL groups (Fig. 1A). The mean pixel gray-scale levels of the control and non-targeted BL thrombi were not significantly different. However, the mean pixel gray-scale level of the thrombi in the targeted BL group was significantly higher than those in the control and non-targeted BL thrombus groups (93 ± 26 vs. 58 ± 16, 48 ± 9, $p = 0.0001$, $n = 10$) (Fig. 1B). Enhancement of ultrasonic thrombus imaging in the targeted BL group lasted at least 15 min, at which point observation was discontinued. BL diameter was 0.185 ± 0.044 μm.

3.2. Scanning electron microscopic observation of thrombi

Large amounts of targeted BL were attached to the fibrin nets and platelets on the surface of thrombi, as well as in the deep inner portions of thrombi (Fig. 2C). In contrast, no BL were attached to the thrombi in the non-targeted BL and control groups (Fig. 2A and B). Targeted BL were smaller than the fibrin mesh (<0.2 μm) in all observed fields.

3.3. In vivo thrombus imaging

The rabbit ilio-femoral arterial thrombus was clearly visualized using a conventional ultrasound system with the targeted BL (Fig. 3A). After targeted BL injection, the mean pixel gray-scale level of the thrombus rapidly peaked (within 1 min) and then gradually decreased; however, it did not return to baseline levels, even after 10 min (Fig. 4). Targeted BL significantly increased the mean pixel gray-scale level of the thrombus at 1 min when compared to that before targeted BL administration (33.2 ± 6.4 vs. 24.8 ± 8.5, $p = 0.0051$, $n = 10$). After non-targeted BL injection, blood echo intensity around the thrombus was increased; however, no significant increases were observed in the

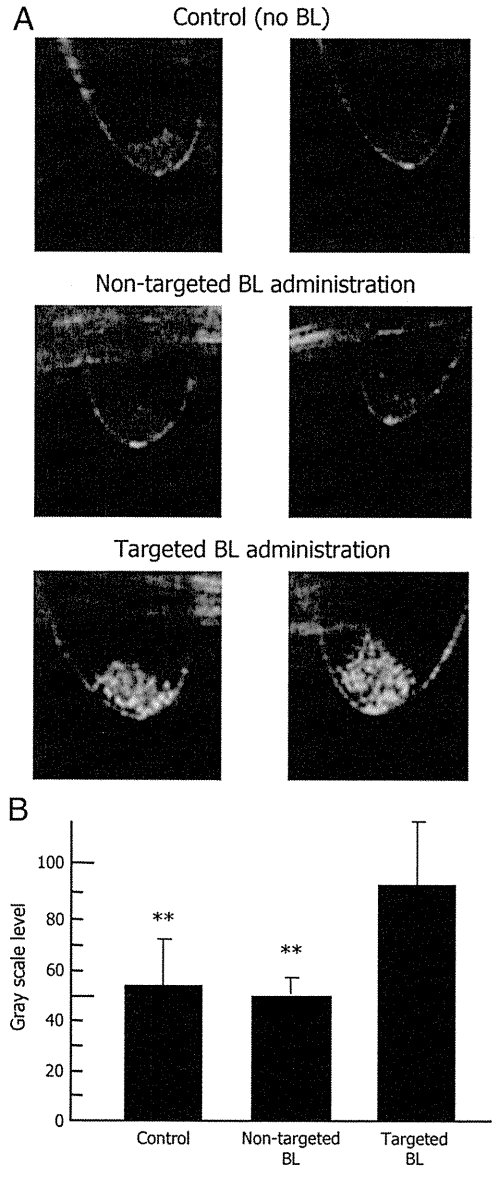

Fig. 1. Ultrasonic thrombus imaging is apparently enhanced by targeted BL *in vitro* when compared to control and non-targeted BL (A). Video intensity levels of the thrombi in the targeted BL group were significantly higher than in the control and non-targeted BL groups (B). BL: bubble liposomes.

mean pixel gray-scale level of the thrombus at 1 min (25.5 ± 4.8 vs. 26.4 ± 5.3, $p = 0.3329$, $n = 10$) (Fig. 3B and C).

4. Discussion

In our *in vitro* and *in vivo* studies, we confirmed that ultrasound imaging of thrombi is markedly enhanced by targeted BL, even via intravenous administration using a conventional diagnostic ultrasound machine. This is also the first study to show the feasibility of perfluorocarbon gas-containing liposomes, rather than a phospholipid mono-layer, as a targeted ultrasound contrast agent, in addition to a carrier for gene delivery [11–13].

In clinical settings, various ultrasound contrast agents with lipid-based or non-lipid-based shells are commercially available for diagnostic use. These agents are prepared to enhance blood flow or tissue perfusion. Some of these agents are capable of passively imaging inflammation using the inherent chemical properties of the shell components [22]. However, they have no specific ligands on their surface for actively targeting pathophysiological molecules.

Lanza et al. first reported a fibrin-targeting ultrasonic contrast agent. They used lipid-encapsulated, nongaseous perfluorocarbon emulsion and an antifibrin monoclonal antibody as a targeting ligand, incorporating avidin-biotin triphasic interaction steps to demonstrate excellent thrombus enhancement [4]. However, this technique has limited applications in humans due to the complexity of targeting interactions and immunogenicity of avidin [23]. Unger et al. developed thrombus-targeting perfluorocarbon gas-containing microbubbles with lipid mono-layer shells incorporating small peptides as ligands for activated platelets [5–7]. This agent was able to enhance ultrasonic thrombus imaging both *in vitro* and *in vivo* during continuous intravenous infusion. Demos and Hamilton reported thrombus-targeting nongaseous echogenic immuno-liposomes, which enhanced ultrasonic imaging of both intravascular and intracardiac thrombi [8,9]. In this study, anti-fibrinogen antibody was used as the targeting ligand, which may cause systemic adverse effects due to secondary immunoreactions. Alonso et al. developed abciximab, an antibody fragment specific for the glycoprotein IIb/IIIa receptor, bearing immunobubbles with phospholipid mono-layer shells. These immunobubbles improved visualization of human clots both *in vitro* and in an *in vivo* model of acute arterial thrombotic occlusion [10].

Targeted BL shows some advantages over these previously reported thrombus-targeting ultrasound contrast agents [4–10]. We used liposomes as a basic structure, as a lipid bi-layer shell increases the stability of BL and works as a barrier against gas diffusion [12], and the liposomal surface can be modified for the conjugation of various targeted ligands, as well as for achieving longer circulation times. Polyethylene glycol was attached to the surface lipid layer in order to

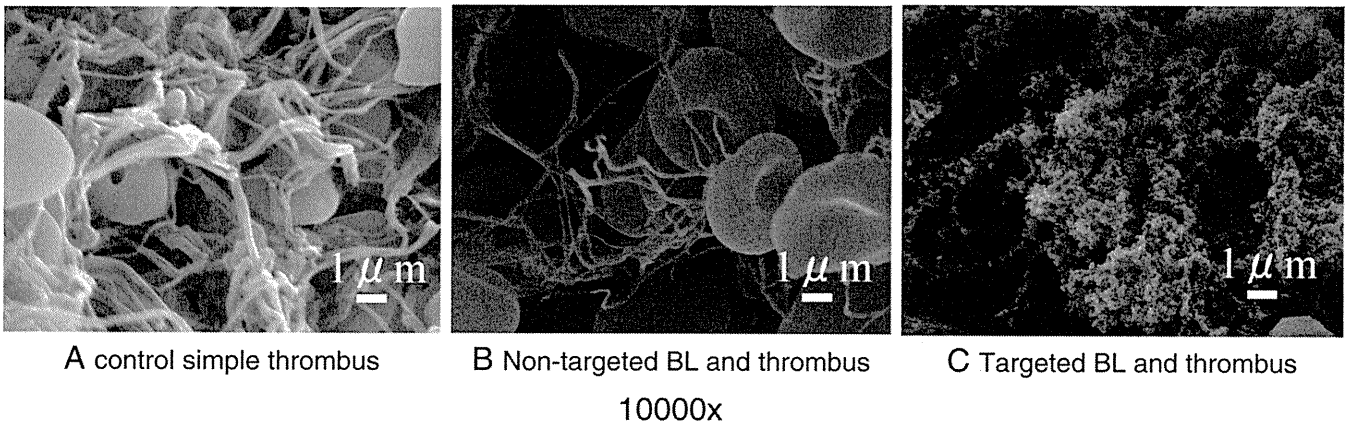

Fig. 2. Scanning electron microscopy revealed large amounts of BL attached to the thrombi in the targeted BL group (C), which were not observed in the non-targeted BL (B) and control groups (A). BL: bubble liposomes.

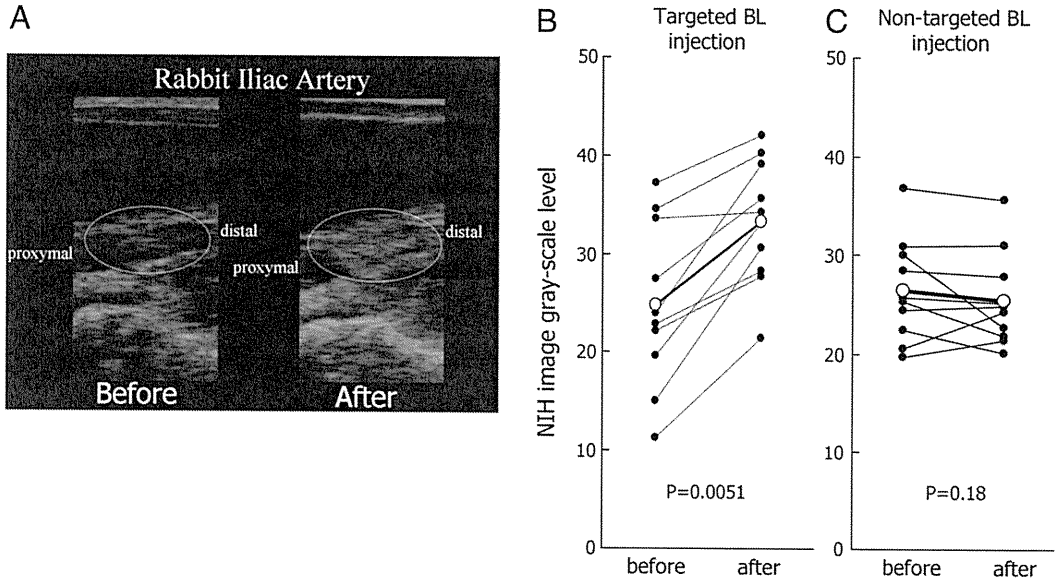

Fig. 3. Ultrasound image of *in vivo* thrombi is significantly enhanced after administration of targeted BL via an ear vein. (A) NIH image quantitative analysis shows significant increases on *in vivo* thrombus echo intensity by intravenous administration of targeted BL; (B) however, similar changes are not seen after administration of non-targeted BL (C). BL: bubble liposomes.

increase hydrophilicity, thereby offering a stealth effect with respect to reticulo-endothelial capture and allowing longer circulation times [24,25]. Moreover, a BL size of less than a micron (nano-size) permits deeper penetration into thrombi.

The targets of ultrasonic thrombus imaging have been fibrin [4,8,9] or activated platelets [5–7,10]. Fibrin is typically present in all types of thrombi (arterial and venous, acute and chronic). In contrast, activated platelets are found in fresh thrombi in cases of acute coronary syndrome and stroke. The RGD sequence-containing peptide is a ligand for the activated platelet membrane glycoprotein IIb/IIIa complex. The RGD peptide is chemically stable and easily conjugated to the lipid surface layer, as it is composed of a small number of amino acids and binds strongly to phospholipids via a thio-ether bond without the need for complex chemical synthesis [14,15]. In contrast to antibodies, peptides are generally smaller in size and simpler in structure, resulting in less immunoreactivity [26,27]. Among the various types of RGD peptides, we used an octapeptide (CGGGRGDF) in this study. The initial C of this peptide was used for coupling and GGG served as an "arm" to distance the active RGD binding site from thiol-coupling to maleimide on the liposomal surface [17]. Moreover, this peptide has been reported to be a potent inhibitor of platelet agglutination through the glycoprotein IIb/IIIa receptor, and to be uniquely sensitive to the activation state of this receptor, even after incorporation into liposomes with polyethylene glycol modification [14,17].

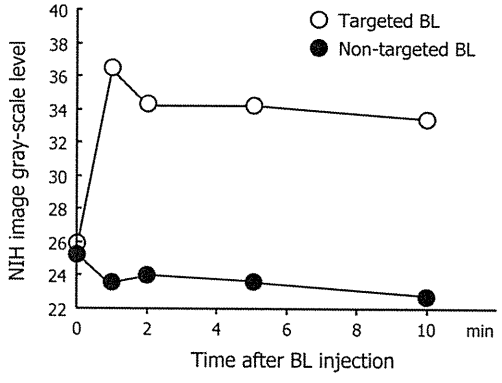

Fig. 4. Representative time-intensity curves of thrombi video intensity immediately before and after targeted and non-targeted BL injection measured using NIH image. Targeted BL significantly increased the mean pixel gray-scale level of the thrombus from 1 to 10 min after injection; however, no significant increases were observed after non-targeted BL injection. BL: bubble liposomes.

The mean diameter of this targeted BL was 0.18 μm. Theoretically, a single BL of this size is out of the diagnostic range of conventional ultrasound imaging. However, BL are apparently echogenic and are clearly visualized with high echo-intensity using conventional ultrasound machines [11]. As shown in the scanning electron microscopic section of this study, the targeted BL accumulated deep within the inner portions of the thrombi, as well as on the surface. This may have been due to the apparently smaller size of BL relative to the space between fibrin nets, and could also explain the strong enhancement on ultrasonic imaging both *in vitro* and *in vivo*. Non-targeted BL were unable to enhance thrombus imaging, probably due to the insufficient amount of BL passively retained around and within the thrombi required for echogenicity.

Liposomes are usually considered nontoxic unless administered at very high doses [28]. Liposomal drugs are already commercially available and are safely used in humans [29–31]. Polyethylene glycol is also considered nontoxic and is excreted unmetabolized in the urine [32]. The RGD peptide is an octapeptide and is considered to be non-toxic and non-immunogenic [26,27]. Perfluoropropane is an inert gas, used as a constituent of commercially available echo contrast agents such as Optison and Definity [33], and is exhaled from the lungs [34]. Therefore, this echo contrast agent is generally considered nontoxic, although safety in humans remains to be demonstrated. Other potential barriers for clinical use are related to the specificity of the RGD peptide. This ligand is highly specific to activated platelet glycoprotein IIb/IIIa receptor [14,17]. However, the specificity is limited and this ligand may also bind to sites of angiogenesis, inflammation, osteoporosis and cancer [35]. In contrast, the relatively high specificity of this ligand to activated platelets may prevent the attachment of the targeted BL to organized chronic thrombi, although this hypothesis was not examined in the present experiment. Therefore, this agent may only enhance fresh thrombi on imaging and may provide a unique opportunity to distinguish fresh thrombi from old organized thrombi. Another limitation of this study is that we did not use the harmonic imaging technique, which is considered to improve ultrasound image quality, particularly when used with echo contrast agents. With the use of harmonic imaging, more distinct enhancement of thrombi can be expected in larger animals or humans.

In conclusion, perfluorocarbon gas-containing liposomal bubbles with RGD peptides are a novel echo contrast agent that can markedly enhance fresh thrombi on ultrasonic imaging *in vitro* and *in vivo*, and may be useful for noninvasive diagnosis of acute thrombotic vessel occlusion.

Acknowledgements

This study was supported in part by a Grant-in-Aid for Scientific Research (B) (16300176) from the Japan Society for the Promotion of Science and a Japan Heart Foundation Research Grant.

The authors of this manuscript have certified that they comply with the Principles of Ethical Publishing in the International Journal of Cardiology [36].

References

[1] Masses, tumors, and source of embolus. In: Feigenbaum H, Armstrong WF, Ryan T, editors. Feigenbaum's echocardiography. 6th ed. Philadelphia, PA: Lippincott Williams & Wilkins; 2005. p. 701–34.
[2] Rose SC, Zwiebel WJ, Murdock LE, et al. Insensitivity of color Doppler flow imaging for detection of acute calf deep venous thrombosis in asymptomatic postoperative patients. J Vasc Interv Radiol 1993;4:111–7.
[3] Popma JJ. Coronary arteriography and intravascular imaging. In: Libby P, Bonow RO, Mann DL, Zipes DP, editors. Braunwald's heart disease: a textbook of cardiovascular medicine. 8th ed. Philadelphia, PA: Saunders Elsevier; 2008. p. 495–6.
[4] Lanza GM, Wallace KD, Scott MJ, et al. A novel site-targeted ultrasonic contrast agent with broad biomedical application. Circulation 1996;94:3334–40.
[5] Unger EC, McCreery TP, Sweitzer RH, Shen D, Wu G. In vitro studies of a new thrombus-specific ultrasound contrast agent. Am J Cardiol 1998;81:58G–61G.
[6] Wu Y, Unger EC, McCreery TP, et al. Binding and lysing of blood clots using MRX-408. Invest Radiol 1998;33:880–5.
[7] Takeuchi M, Ogunyankin K, Pandian NG, et al. Enhanced visualization of intravascular and left atrial appendage thrombus with the use of a thrombus-targeting ultrasonographic contrast agent (MRX-408A1): in vivo experimental echocardiographic studies. J Am Soc Echocardiogr 1999;12:1015–21.
[8] Demos SM, Alkan-Onyuksel H, Kane BJ, et al. In vivo targeting of acoustically reflective liposomes for intravascular and transvascular ultrasonic enhancement. J Am Coll Cardiol 1999;33:867–75.
[9] Hamilton A, Huang SL, Warnick D, et al. Left ventricular thrombus enhancement after intravenous injection of echogenic immunoliposomes: studies in a new experimental model. Circulation 2002;105:2772–8.
[10] Alonso A, Della Martina A, Stroick M, et al. Molecular imaging of human thrombus with novel abciximab immunobubbles and ultrasound. Stroke 2007;38:1508–14.
[11] Suzuki R, Takizawa T, Negishi Y, et al. Gene delivery by combination of novel liposomal bubbles with perfluoropropane and ultrasound. J Control Release 2007;117:130–6.
[12] Suzuki R, Takizawa T, Negishi Y, et al. Tumor specific ultrasound enhanced gene transfer in vivo with novel liposomal bubbles. J Control Release 2008;125:137–44.
[13] Suzuki R, Takizawa T, Negishi Y, Utoguchi N, Maruyama K. Effective gene delivery with liposomal bubbles and ultrasound as novel non-viral system. J Drug Target 2007;15:531–7.
[14] Gyongyossy-Issa MIC, Muller W, Devine DV. The covalent coupling of Arg-Gly-Asp-containing peptides to liposomes: purification and biochemical function of the lipopeptide. Arch Biochem Biophys 1998;353:101–8.
[15] Nishiya T, Sloan S. Interaction of RGD liposomes with platelets. Biochem Biophys Res Commun 1996;224:242–5.
[16] Szoka Jr F, Papahadjopolus D. Procedure for preparation of liposomes with large internal aqueous space and high capture by reverse-phase evaporation. Proc Natl Sci U S A 1978;75:4194–8.
[17] Beer JH, Springer KT, Coller BS. Immobilized Arg-Gly-Asp (RGD) peptides of varying lengths as structural probes of the platelet glycoprotein IIb/IIIa receptor. Blood 1992;79:117–28.
[18] NIH image home page. http://rsb.info.nih.gov/nih-image/ Accessed January 29, 2010.
[19] Glauert AM, Lewis PR. Biological specimen preparation for transmission electron microscopy. In: Glauert AM, editor. Practical methods in electron microscopy Volume 17. London, UK: Portland Press; 1998.
[20] Steffen W, Fishbein MC, Luo H, et al. High intensity, low frequency catheter-delivered ultrasound dissolution of occlusive coronary artery thrombi: an in vitro and in vivo study. J Am Coll Cardiol 1994;24:1571–9.
[21] Nishioka T, Luo H, Fishbein MC, et al. Dissolution of thrombotic arterial occlusion by high intensity, low frequency ultrasound and dodecafluoropentane emulsion: an in vitro and in vivo study. J Am Coll Cardiol 1997;30:561–8.
[22] Lindner JR. Microbubbles in medical imaging: current applications and future directions. Nature Rev Drug Discov 2004;3:527–32.
[23] Lanza GM, Wickline SA. Targeted ultrasonic contrast agents for molecular imaging and therapy. Curr Probl Cardiol 2003;28:625–53.
[24] Klibanov AL, Maruyama K, Torchilin VP, Huang L. Amphipathic polyethyleneglycols effectively prolong the circulation time of liposomes. FEBS Lett 1990;268:235–7.
[25] Maruyama K, Yuda T, Okamoto A, Kojima S, Suginaka A, Iwatsuru M. Prolonged circulation time in vivo of large unilamellar liposomes composed of distearoyl phosphatidylcholine and cholesterol containing amphipathic poly(ethylene glycol). Biochim Biophys Acta 1992;1128:44–9.
[26] Lee TY, Lin CT, Kuo SY, Chang DK, Wu HC. Peptide-mediated targeting to tumor blood vessels of lung cancer for drug delivery. Cancer Res 2007;67:10958–65.
[27] Chang DK, Lin CT, Wu CH, Wu HC. A novel peptide enhances therapeutic efficacy of liposomal anticancer drugs in mice models of human lung cancer. PLoS ONE 2009;4:e4171.
[28] Storm G, Oussoren C, Peelers PAM, Barenholz Y. Tolerability of liposomes *in vivo*. In: Gregoriadis G, editor. Liposome technology. Boca Raton, FL: CRC Press, Inc.; 1993. p. 345–83.
[29] Davidson RN, Croft SL, Scott A, Maini M, Moody AH, Bryceson AD. Liposomal amphotericin B in drug-resistant visceral leishmaniasis. Lancet 1991;337:1061–2.
[30] Guaglianone P, Chan K, DelaFlor-Weiss E, et al. Phase I and pharmacologic study of liposomal daunorubicin (DaunoXome). Invest New Drugs 1994;12:103–10.
[31] Gabizon A, Peretz T, Sulkes A, et al. Systemic administration of doxorubicin-containing liposomes in cancer patients: a phase I study. Eur J Cancer Clin Oncol 1989;25:1795–803.
[32] Carpenter CP, Woodside MD, Kinkead ER, King JM, Sullivan LJ. Response of dogs to repeated intravenous injection of polyethylene glycol 4000 with notes on excretion and sensitization. Toxicol Appl Pharmacol 1971;18:35–40.
[33] Wei K, Mulvagh SL, Carson L, et al. The safety of Definity and Optison for ultrasound image enhancement: a retrospective analysis of 78, 383 administered contrast doses. J Am Soc Echocardiogr 2008;11:1202–6.
[34] Hutter JC, Luu HM, Mehlhaff PM, Killam AL, Dittrich HC. Physiologically based pharmacokinetic model for fluorocarbon elimination after the administration of an octafluoropropane-albumin microsphere sonographic contrast agent. J Ultrasound Med 1999;18:1–11.
[35] Meyer A, Auernheimer J, Modlinger A, Kessler H. Targeting RGD recognizing integrins: drug development, biomaterial research, tumor imaging and targeting. Curr Pharm Des 2006;12:2723–47.
[36] Coats AJ. Ethical authorship and publishing. Int J Cardiol 2009;131:149–50.